Toxicology and Applied Pharmacology 352 (2018) 59–67

Contents lists available at ScienceDirect

Toxicology and Applied Pharmacology

journal homepage: www.elsevier.com/locate/taap

Membrane cholesterol delays cellular apoptosis induced by ginsenoside Rh2, a steroid saponin

Sandrine L. Verstraeten[a,b], Marie Albert[a], Adrien Paquot[c], Giulio G. Muccioli[c], Donatienne Tyteca[b], Marie-Paule Mingeot-Leclercq[a,*]

[a] Louvain Drug Research Institute (LDRI), Cellular & Molecular Pharmacology Unit (FACM), Université catholique de Louvain (UCL), Brussels 1200, Belgium
[b] de Duve Institute (DDUV), Cell Biology Unit (CELL), Université catholique de Louvain (UCL), Brussels 1200, Belgium
[c] Louvain Drug Research Institute (LDRI), Bioanalysis and Pharmacology of Bioactive Lipids Research Group (BPBL), Université catholique de Louvain (UCL), Brussels 1200, Belgium

ARTICLE INFO

Keywords:
Ginsenoside
Saponin
Cholesterol
Membrane
Apoptosis
Akt

ABSTRACT

Saponins exhibit several biological and pharmacological activities, such as antibacterial, anti-inflammatory and anticancer effects. Many studies attribute their activities to their interactions with cholesterol. In this study, we focus on the steroid saponin ginsenoside Rh2, one of the active principles of *Panax ginseng* root. Some evidence suggests that lipid rafts, defined as nanodomains enriched in cholesterol and sphingolipids, could be involved in the Rh2-induced apoptosis. However, the role of membrane lipids, especially cholesterol, in this process is still poorly understood. Here, we demonstrate that (i) A549, THP-1 and U937 cells are all susceptible to the Rh2-induced apoptosis but to a differential extent and (ii) the cytotoxic effect inversely correlates with the cell membrane cholesterol content. Upon cholesterol depletion via methyl-β-cyclodextrin, those three cells lines become more sensitive to Rh2-induced apoptosis. Then, focusing on the cholesterol-auxotroph U937 cell line, we showed that Rh2 alters plasma membrane fluidity by compacting the hydrophobic core of lipid bilayer (DPH anisotropy) and relaxing the interfacial packaging of the polar head of phospholipids (TMA-DPH anisotropy). The treatment with Rh2 conducts to the dephosphorylation of Akt and the activation of the intrinsic pathway of apoptosis (loss of mitochondrial membrane potential, caspase-9 and -3 activation). All these features are induced faster in cholesterol-depleted cells, which could be explained by faster cell accumulation of Rh2 in these conditions. This work is the first reporting that membrane cholesterol could delay the activity of ginsenoside Rh2, renewing the idea that saponin cytotoxicity is ascribed to an interaction with membrane cholesterol.

1. Introduction

Saponins, mainly produced by plants, are widely used in medicine for their multiple biological and pharmacological activities including immunomodulatory, anti-inflammatory or anti-cancer (Lorent et al., 2014a). Cytotoxic and hemolytic activities for most saponins (e.g. digitonin (Korchowiec et al., 2015; Sudji et al., 2015; Frenkel et al., 2014), α-tomatine (Keukens et al., 1996), α-hederin (Lorent et al., 2016; Lorent et al., 2014b), seem to be ascribed to their ability to interact with membrane lipids, especially cholesterol (de Groot and Muller-Goymann, 2016). For example, digitonin induces membrane permeability in the presence of cholesterol by removing cholesterol from the membrane and forming complexes with the latter (Sudji et al., 2015).

Cholesterol plays a crucial role in the stability, dynamics and organization of the plasma membrane, serving as a spacer between hydrocarbon chains of phospho- and sphingo-lipids (Ikonen, 2008). It is distributed heterogeneously in the plasma membrane (Carquin et al., 2016), notably enabling the formation of "lipid rafts" (Simons and Sampaio, 2011; Lingwood and Simons, 2010; Simons and Ikonen, 1997), transient ordered nanometric domains enriched in cholesterol and sphingolipids. Rafts are proposed to serve as platforms capable of promoting various cellular signaling including pro- and anti-apoptotic pathways such as the Fas death receptor and the phosphatidylinositol-3 kinase (PI3K)/Akt cell survival pathways, respectively (George and Wu, 2012; Mollinedo and Gajate, 2015).

Among steroid saponins, ginsenosides are the active components of ginseng, a well-known chinese medicinal plant. More than hundreds of different ginsenosides have been isolated from ginseng and have shown in the past to be membrane active substances and to influence the

* Corresponding author at: FACM/LDRI-UCL – Cellular and Molecular Pharmacology Unit of the Louvain Drug Research Institute, Université catholique de Louvain, Avenue E. Mounier 73, B1.73.05, B-1200 Brussels, Belgium.
E-mail address: marie-paule.mingeot@uclouvain.be (M.-P. Mingeot-Leclercq).

https://doi.org/10.1016/j.taap.2018.05.014
Received 19 December 2017; Received in revised form 4 May 2018; Accepted 14 May 2018
Available online 18 May 2018
0041-008X/

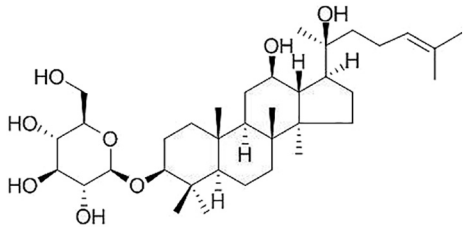

Fig. 1. The chemical structure of the ginsenoside Rh2, a steroid saponin.

membrane by modulating lipid membrane dynamics (Qi et al., 2011; Tsuchiya, 2015; Kwon et al., 2008). In this study, we focus on the ginsenoside Rh2 (Fig. 1), phytosterol from *Panax ginseng*. To the best of our knowledge, only two studies have reported the disruption of lipid rafts by Rh2 leading to apoptosis, via either the FAS oligomerization in Hela cells (Yi et al., 2009) or inactivation of Akt in human epidermoid carcinoma A431 cells and in human breast cancer MBA-MB-231 cells (Park et al., 2010). Taken together, these data suggest that rafts could be involved in Rh2-induced apoptosis. However, mechanistic understanding of the mode of interactions between Rh2 and membrane lipids and the exact subsequent apoptotic pathways are still poorly understood.

Since lipid rafts are enriched in cholesterol and since some saponins have been shown to interact with cholesterol, the aim of the present study was to explore the role of membrane cholesterol in the cytotoxic activity of Rh2. To this end, we used three cell lines exhibiting differential membrane cholesterol level: carcinomic human alveolar basal epithelial A549 > human monocytic leukemia THP-1 > U937 cells. We demonstrated that Rh2 induced apoptosis in a concentration- and time-dependent manner in the three cell lines. More importantly, A549, THP-1 and U937 cells can be classified from the more resistant to the more susceptible to the Rh2-induced apoptosis. In addition, upon cholesterol depletion via methyl-β-cyclodextrin (MβCD), those three cell lines became more sensitive to Rh2-induced apoptosis. To explore the mechanistic behind this observation, we then focused on the cholesterol-auxotroph U937 cell line (Billheimer et al., 1987). We showed that Rh2 altered plasma membrane fluidity, induced Akt dephosphorylation and the activation of the intrinsic pathway of apoptosis. Fluidity changes, Akt dephosphorylation and apoptosis appeared faster in cholesterol-depleted cells, which could be explained by a faster cell accumulation of Rh2 in these conditions.

This work is the first reporting that membrane cholesterol could delay the activity of ginsenoside Rh2, renewing the idea that saponin cytotoxicity is only ascribed to an interaction with membrane cholesterol.

2. Materials and methods

2.1. Cells and materials

Ginsenoside Rh2, methyl-β-cyclodextrin (MβCD), ethidium bromide, acridine orange, 4′,6-diamidino-2-phenylindole (DAPI), digoxin, 1,6-diphenyl-1,3,5-hexatriene (DPH), protease and phosphatase inhibitor cocktails and *Bacillus cereus* sphingomyelinase (SMase) were purchased from Sigma-Aldrich (St. Louis, MO, USA). U937, THP-1 and A549 cell lines were purchased from ATCC. RPMI-1640 medium and trypsin were ordered from Life technologies (Paisley, SL, UK). Delipidated serum was purchased from Labconsult (BE). Blue trypan, bicinchoninic protein assay, caspase-9 colorimetric assay kit, JC-1, NuPAGE reagents, PVDF membrane, Supersignal West Pico and Amplex® red cholesterol assay kit were purchased from Thermo scientific (Rockford, IL, USA). 1-(4-trimethylammoniumphenyl)-6-phenyl-1,3,5-hexatriene (TMA-DPH) was ordered from Molecular Probes (Eugene, OR, USA). Caspase-9 inhibitor (*Z*-LEHD-FMK) was purchased from R & D System (Minneapolis, MN, USA). Anti-phospho-Akt (Ser^{473}) (#4060) and anti-Akt (#9272) were purchased from Cell Signaling Technology (Beverly, MA, USA). Anti-β actin (sc-47778) and anti-caspase-3 (sc-7148) were purchased from Santa Cruz Biotechnology (Santa Cruz, CA, USA). TLC silica gel 60F was purchased from Merck Millipore (Billerica, MA, USA). All other reagents were purchased from VWR International (Atlanta, GA, USA) and were of analytical grade.

2.2. Cell culture and incubation with ginsenoside Rh2

Cells were cultured in suspension in RMPI-1640 medium supplemented with 10% fetal calf serum at 37 °C in 5% CO_2. Ginsenoside Rh2 was dissolved in absolute ethanol. After evaporation of the solvent, the residue was resolubilized in RPMI-1640 medium supplemented with 10% delipidated serum containing 0.1% DMSO in an ultrasonic bath for 5 min. Cells were incubated with 60 μM ginsenoside Rh2 (unless otherwise stated) in RMPI-1640 medium with 10% delipidated serum to avoid interaction between Rh2 and lipids in the serum and to prevent cholesterol and sphingomyelin replenishment at the membrane after cholesterol and sphingomyelin depletion with MβCD and SMase, respectively. After treatment with Rh2, cells were washed twice in Phosphate Buffered Saline (PBS) (10 mM Na_2HPO_4, 137 mM NaCl and 2.7 mM KCl).

2.3. Plasma membrane cholesterol or sphingomyelin depletion and assay

In serum-free RPMI-1640 supplemented with 1 mg/ml BSA, THP-1 cells were treated with 3 mM MβCD for 2 h whereas A549 and U937 cells were treated with 5 mM MβCD for 45 min and 2 h, respectively. In some experiments, U937 were also treated with raising concentration of MβCD (0 to 7 mM) for 2 h or SMase (0 to 60 mU/ml) for 1 h. Cells were then washed with serum-free RPMI and incubated with Rh2 for the indicated times. After the treatment with MβCD, cells were directly quantified for their cholesterol by the Amplex® red cholesterol assay and phospholipid contents by phosphorus assay after lipid extraction (Gamble et al., 1978; Bartlett, 1959). The ratio of cholesterol/phospholipid was determined and expressed by reference to the control. To evaluate sphingomyelin content, lipids were directly extracted after SMase treatment (Bartlett, 1959), separated on silica gel TLC plates in chloroform:methanol:$CaCl_2$ (15 mM) (65:35:8; v/v/v) and detected by charring in the presence of 10% cupric sulfate in 8% O-phosphoric acid (Kritchevsky et al., 1973; Carquin et al., 2014). Band intensity of sphingomyelin was quantified and expressed by reference to bands corresponding to phospholipids from the same sample and then expressed as percentage of control.

2.4. Apoptotic/non-apoptotic cell death

DAPI assay was carried out to quantify apoptosis as previously described (Servais et al., 2006). Briefly, cells presenting a fragmented and condensed nucleus were counted as apoptotic. Data were expressed as the percentage of apoptotic nuclei relative to total number of nuclei counted. A total number of 200 cells was counted per sample. Acridine orange/ethidium bromide (AO/EB) assay was performed to distinguish between living, death cells and early and late apoptotic cells (Kasibhatla et al., 2006). After treatment with Rh2, cells were incubated with the AO/EB solution and directly observed by fluorescence microscopy. A total number of 200 cells was counted per sample.

2.5. Trypan blue exclusion assay

Cell death was quantified by the trypan blue exclusion assay. Cells colored in trypan blue were considered as non-viable and the percentage of non-viable cells was calculated as the number of death cells divided by the total number of cells.

2.6. Quantification of intracellular ginsenoside Rh2 by HPLC MS/MS

After treatment with ginsenoside Rh2, cell pellets were resuspended in H_2O and digoxin (internal standard; 1 mg/ml) was added. Cells were lysed by sonication for 10 min and proteins were precipitated by adding a mixture of acetonitrile and methanol (MeOH) (21:4, v/v). After 20 min at −20 °C, lysates were centrifuged at 11,000 *g* for 5 min at room temperature. Supernatants were collected and dried. The dried samples were reconstituted in MeOH:H_2O (1:1, v/v) and injected on a Supelcosil LC-18 (150 × 4 mm; 3 μm) column preceded by a C-18 Supelguard precolumn maintained at 25 °C. Tandem quadrupole mass spectrometry was used to detect the ginsenoside Rh2 and digoxin. The negative ionization mode was selected for analysis. The mobile phase A consisted in MeOH:H_2O (1:1, v/v) and the mobile phase B was 100% MeOH (both containing 0.1% NH_4OH). The gradient consisted in a linear increase from 0% B to 100% B in 7.5 min followed by a 7.5 min plateau maintained before requilibrating the column. The data analysis was achieved by using the *MassLynx® software* to integrate peaks corresponding to the quantification transitions selected for the ginsenoside Rh2 (621.4 → 160.9) and for the digoxin (779.4 → 85.0). Qualification transitions were also used for both ginsenoside Rh2 (621.4 → 459.4) and digoxin (779.4 → 519.3) to further confirm the nature of the peak analyzed. The ratio of the area under the curve (AUC) of ginsenoside over the AUC of digoxin was determined and the amount of Rh2 in the cells was calculated using a calibration curve. Nine calibration solutions ranging between 0 and 60 pmol (on column) were prepared and the slope (0.056), intercept (0.029) and coefficient of determination (R^2: 0.9981) of the calibration curve were determined. Based on the calibration curve, the LOD and LOQ were also determined and found to be 0.0095 pmol and 0.0445 pmol on column, respectively. The accuracy expressed as bias (in %) was determined at four levels ranging from 0.117 to 60 pmol. The values were included between 0.006% and 0.097. The intracellular accumulation of Rh2 was then reported to the total protein amount determined by the BCA method using bovine serum albumin as a standard.

2.7. Plasma membrane fluidity

DPH or TMA-DPH were dissolved in tetrahydrofuran at a concentration of 2 mM. After incubation with Rh2, cells were washed and mixed with 2 μM DPH or TMA-DPH dispersed in PBS for 30 min or 5 min at 37 °C in the dark, respectively. The fluorescence anisotropy values (r) were determined using the equation:

$$(r) = (I_{vv} - G.\ I_{vh})/(I_{vv} + 2.\ G/I_{vh})$$

where Ivv and Ivh are the fluorescence intensities with the excitation and emission polarization filters in vertical (v) and horizontal (h) orientations, respectively. The G factor is an inherent factor to the spectrometer. The fluorescence polarization was measured at 37 °C at excitation and emission wavelengths of 365 nm and 425 nm, respectively, using a LS55 luminescence spectrometer connected to a circulating water bath.

2.8. Western blot

After treatment with Rh2, cells were resuspended in RIPA buffer (25 mM Tris-HCl, pH 7.4; 150 mM NaCl; 1% NP-40; 0.1% SDS; 1% sodium deoxycholate) supplemented with protease and phosphatase inhibitor cocktail. After 15 min on ice, cell lysates were centrifuged for 15 min at 14,000 *g* at 4 °C to pellet any insoluble material. The protein concentration of the supernatant was assessed using the BCA method. Western blots were performed using the NuPAGE electrophoresis system. 50 μg from each sample was mixed to 4× NuPAGE LDS sample buffer and 10× NuPAGE reducing agent, then heated at 70 °C for 10 min. Samples were separated on acrylamide gels (NuPAGE Bis-Tris Gel) and transferred to PVDF membranes (0.45 μm). Membranes were blocked in 5% non-fat dry milk in Tris-buffered saline containing 0.05% Tween-20 (TBST) and then incubated with appropriate diluted primary antibodies (Akt and p-Akt: 1/1000; β-actin and caspase-3: 1/200) at 4 °C overnight. Membranes were washed three times with TBST buffer and exposed to appropriate horseradish peroxidase-coupled secondary antibodies for 1 h. Blots were revealed by chemiluminescence (SuperSignal West Pico).

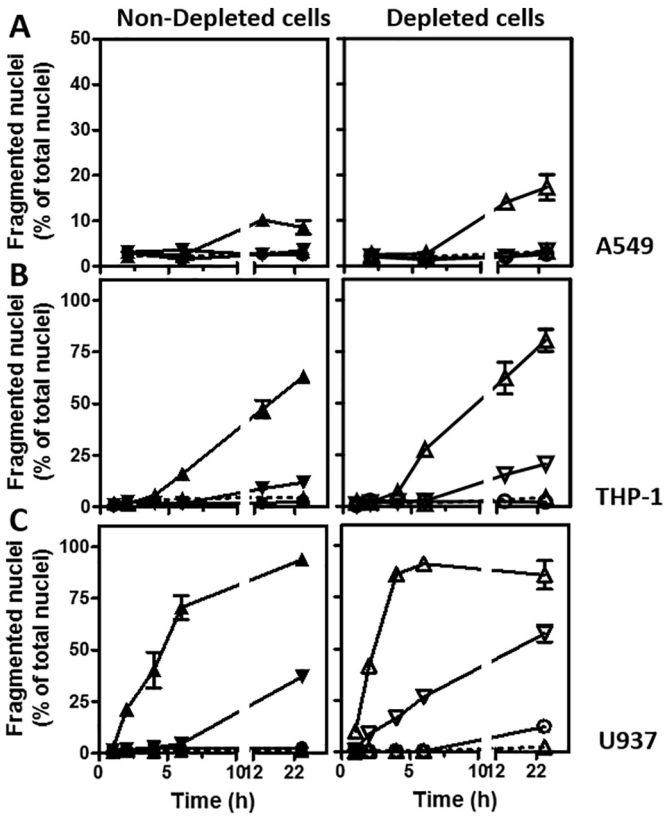

Fig. 2. Ginsenoside Rh2 induces faster cell cytotoxicity upon membrane cholesterol depletion in a concentration-dependent manner. Cells were kept untreated (left panel) or treated with MβCD (right panel). THP-1 (B) were treated with 3 mM for 2 h whereas A549 (A) and U937 (C) cells were treated with 5 mM MβCD for 45 min and 2 h, respectively. Cholesterol-depleted cells with MβCD (open symbol, right panel) or not (closed symbol, left panel) were incubated for the indicated times with increasing concentrations of Rh2: 20 μM (circle), 40 μM (inverted triangle), 60 μM (triangle) or with 0.1% DMSO (vehicle, dotted line, triangle). The number of fragmented nuclei was determined by DAPI. Results are the mean ± SEM of at least two independent experiments performed in triplicate. Where not visible, error bars are included in the symbols.

Table 1
Cellular cholesterol content in cells depleted or not in cholesterol by MβCD. Cells were kept untreated (second column) or treated with MβCD (third column). THP-1 were treated with 3 mM MβCD for 2 h whereas A549 and U937 cells were treated with 5 mM MβCD for 45 min and 2 h, respectively.

Cell lines	Chol (μg/mg protein) Non-depleted	Chol (μg/mg protein) Depleted
A549	34.58 ± 6.36	17.1 ± 7.17
THP-1	20.13 ± 4.04	10.52 ± 3.22
U937	10.68 ± 1.68	5.30 ± 2.95

2.9. Caspase-9 activity

Caspase-9 activity was measured using colorimetric protease assay kit. Briefly, cells treated with Rh2 were washed and resuspended in RIPA lysis buffer for 15 min on ice. After centrifugation (14,000 *g*,

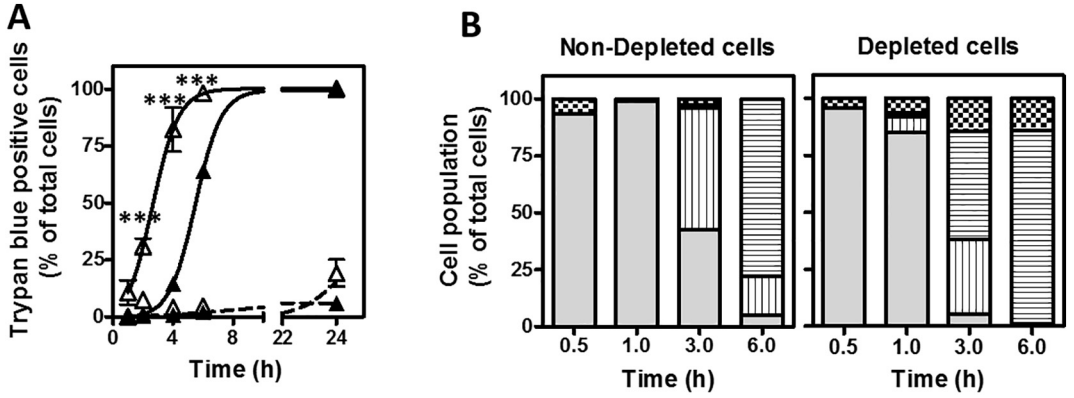

Fig. 3. Ginsenoside Rh2 induces faster U937 cell cytotoxicity upon membrane cholesterol depletion. A, B U937 cells cholesterol-depleted with 5 mM MβCD for 2 h (open triangle) or not (closed triangle) were incubated for the indicated times with 60 μM Rh2 (solid line) or with 0.1% DMSO (vehicle, dotted line). A. The number of dead cells was determined by trypan blue. Results are the means ± SEM of at least three independent experiments performed in triplicate. Two-way ANOVA with Bonferroni post-tests to compare points between non-depleted versus depleted cells treated with Rh2. The lines correspond to a non-linear regression (Hill's function) of data values. B. Cells were stained with acridine orange/ethidium bromide dyes. Staining method distinguished between living cells (grey bars), early apoptosis (vertical bars), late apoptosis (horizontal bars) and necrosis (check board bars). The result is the mean of two independent experiments done in triplicate. Depleted vs non-depleted conditions: ***, $p < 0.001$.

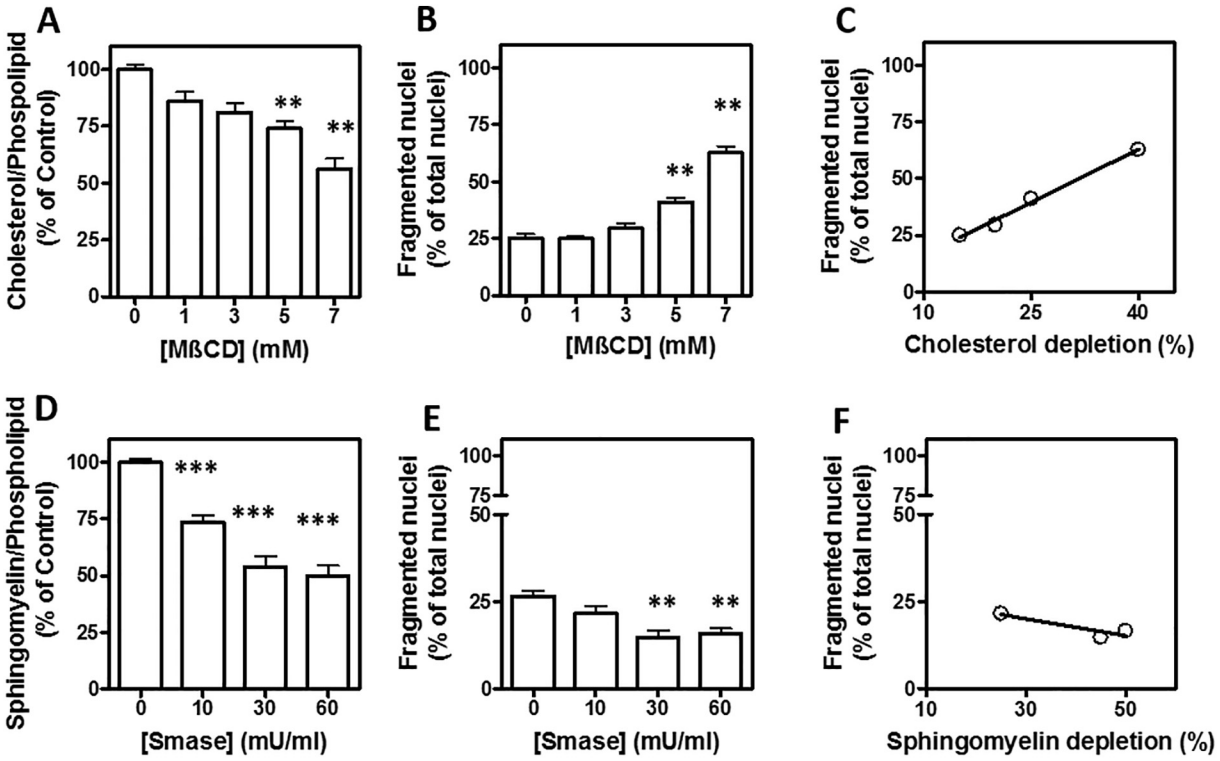

Fig. 4. Ginsenoside Rh2 induces stronger U937 cell cytotoxicity upon membrane cholesterol depletion and the opposite upon membrane sphingomyelin depletion. A, D. U937 cells were treated with raising MβCD (A) or Smase (B) concentrations for 2 h and 1 h, respectively. The cholesterol/phospholipid and sphingomyelin/phospholipid ratios were measured and expressed by reference to the control. One-way ANOVA with Dunnett's post test to compare points for control versus cells incubated with MβCD or Smase. **, $p < 0.01$; ***, $p < 0.001$. B, E. After treatment with increasing MβCD or SMase, cells were exposed for an additional 2 h with 60 μM Rh2 (in the absence of MβCD or SMase) and DAPI assay was performed. The experiment was repeated at least two times independently, each time in triplicate. One way ANOVA with Dunnett's post test. **, $p < 0.01$. C, F. Correlation between the cytotoxicity effect induced by Rh2 and the percentage of cholesterol or sphingomyelin reduction expressed by reference to the control. The line corresponds to a linear regression of data values with $R^2 = 0.99$ or $R^2 = 0.8124$ for cholesterol or sphingomyelin depletion, respectively.

15 min), protein concentration of the supernatants was measured using the BCA method. Amount of 50 μg of proteins diluted in 50 μl of buffer RIPA were mixed with 2× reaction buffer in a 96 well microplate and 5 μl of peptide substrates of caspase-9 (Ac-LEHD-pNA) was added. After 24 h incubation in the dark at 37 °C, the absorbance of the samples was read in a microplate reader at 400 nm. In some experiments, caspase-9 inhibitor (*Z*-LEHD-FMK, 125 μM) was added to fresh medium 1 h before the treatment with Rh2.

2.10. Loss of mitochondrial membrane potential

Loss of mitochondrial membrane potential was determined using the mitochondrial membrane potential sensitive cationic dye JC-1. Briefly, Rh2-treated cells were stained with 10 μM JC-1 for 30 min at

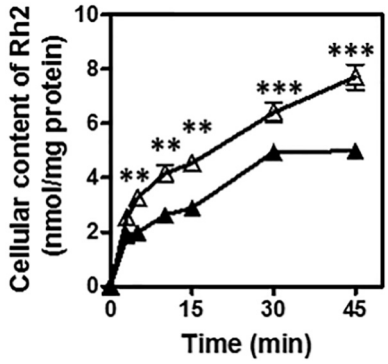

Fig. 5. Uptake of Rh2 by U937 cells is accelerated upon membrane cholesterol depletion. U937 cells were cholesterol-depleted (5 mM MβCD, open triangles) or not (closed triangles) and then incubated with 60 μM Rh2 over time. The amount of Rh2 in cell lysates was measured using HPLC MS/MS and expressed by reference to the amount of proteins. Each symbol is the mean ± SEM of at least three independent experiments done in triplicate. Two-way ANOVA with Bonferroni post-tests to compare points for non-depleted vs depleted cells. **, $p < 0.01$; ***, $p < 0.001$.

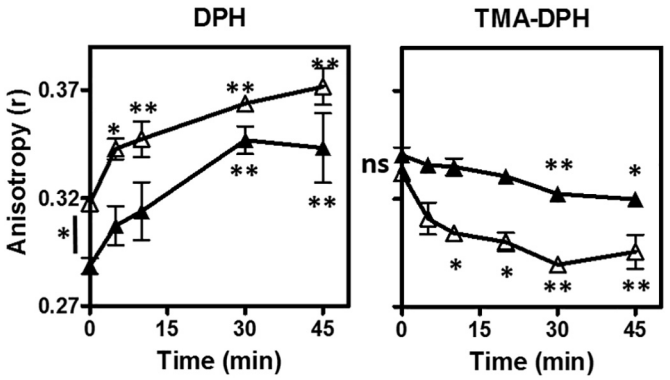

Fig. 6. Rh2 induces faster rigidification of the hydrophobic core (DPH) and fluidification of the interfacial region (TMA-DPH) of the U937 lipid bilayer upon membrane cholesterol depletion. U937 cells non-depleted (closed triangles) or cholesterol-depleted (5 mM MβCD, open triangles) were treated with 60 μM Rh2 at the indicated times and then incubated with DPH (left panel) or TMA-DPH (right panel) for 30 or 5 min, respectively. The anisotropy (r) values were measured. Results are means ± SEM of two independent experiments in triplicate. Student's t-test was performed to compare control depleted and non-depleted cells. One-way ANOVA with Dunnett's post-test to compare control cells vs cells incubated with Rh2. ns, not significant, *, $p < 0.05$; **, $p < 0.01$.

37 °C in the dark. Cells were washed and resuspended with PBS and the fluorescence was detected with a microplate reader at an excitation wavelength of 490 nm and emission wavelengths of 525 and 590 nm.

2.11. Data analysis

Data are expressed as means ± SEM. All statistical analyses were performed with the GraphPad Prism 4.03 software (GraphPad software, San Diego, CA, USA).

3. Results

In a first series of experiments, we examined the time and concentration dependence of the Rh2-induced apoptosis in A549, THP-1 and U937 cells. To this aim, cells were treated with increasing concentrations of Rh2 (20, 40 and 60 μM) for increasing periods of time (1 h to 24 h) and tested for apoptosis by DAPI staining. As shown in the left panel of Fig. 2, the Rh2-induced apoptosis extent was Rh2 concentration- and incubation time- as well as cell line-dependent. For instance, the U937 cell line (C) was more susceptible to the Rh2-induced apoptosis than THP-1 cells (B), themselves more susceptible than A549 cells (A). After 6 h of incubation, 60 μM Rh2 induced ~50% of fragmented nuclei in U937, ~15% in THP-1 without any effect in A549 cells. Since U937, THP-1 and A549 cells exhibited increasing membrane cholesterol (Table 1), those results suggested an inversed correlation between susceptibility to Rh2 and membrane cholesterol content: higher the cholesterol content, lower the Rh2-induced apoptosis. To further test this hypothesis, the same experiment was performed in cells depleted in cholesterol (right panel of Fig. 2). For this purpose, THP-1 were pretreated with 3 mM MβCD, whereas A549 and U937 cells were pretreated with 5 mM MβCD, a cholesterol-sequestering agent (Zidovetzki and Levitan, 2007). Those non-cytotoxic MβCD concentrations reduced by ~50% the ratio of cholesterol/protein in the three cell lines (Table 1). As shown in the right panel of Fig. 2, in all the conditions investigated, cholesterol-depleted cells were more sensitive to Rh2-induced apoptosis, corroborating the idea that a decrease in cholesterol content correlated with an increased number of apoptotic cells induced by Rh2.

To further investigate the role of cholesterol in the Rh2-induced cytotoxicity, we then focused on the U937 cell line, which is cholesterol auxotroph and considered as a valuable model to study the importance of cholesterol in membrane structure and function (Billheimer et al., 1987), and used the effective concentration of 60 μM Rh2. We started by analyzing the effect of Rh2 on membrane permeability and cell death via trypan blue assay. Depletion of cholesterol by MβCD effectively increased and accelerated the Rh2-induced cell death, confirming the results obtained with DAPI staining (Fig. 3A). Noteworthy, the apoptosis was observed before the appearance of cell death in non-depleted cells. Acridine orange/ethidium bromide staining was also performed to visualize membrane permeabilization in parallel with nucleus morphology changes (Lorent et al., 2016). The treatment with Rh2 conducted first to apoptosis observed by nuclear fragmentation followed in a second step by the loss of plasma membrane integrity and necrosis (Fig. 3B). > 45% of the cells lost their membrane integrity after 3 h of incubation with 60 μM of Rh2 in cholesterol-depleted cells while this phenomenon was not yet observed in non-depleted cells. In all the conditions investigated, depletion of cholesterol accelerated the cytotoxic effect of Rh2.

To confirm the protective role of membrane cholesterol in the Rh2-induced apoptosis, U937 cells were pretreated with 0 to 7 mM MβCD. Upon treatment with 5 mM and 7 mM MβCD, the cholesterol/phospholipid ratio was reduced to ~75% and 60% of that of control cells, respectively (Fig. 4A). Cells with varying contents of cholesterol were then treated with 60 μM Rh2 for 2 h and DAPI assay was performed to determine the percentage of fragmented nuclei (Fig. 4B). As expected, the increase of membrane cholesterol depletion via the pretreatment with raising concentrations of MβCD correlated with an increased number of apoptotic cells following Rh2 treatment (Fig. 4C). These data confirm that lower the cholesterol level is, higher the Rh2-induced apoptosis is. To determine whether those effects are specific to membrane cholesterol depletion, cells were incubated with 0 to 60 mU/ml *Bacillus cereus* sphingomyelinase (SMase) for sphingomyelin depletion. In these conditions, the reduction of sphingomyelin content reached ~50% of that of control cells (Fig. 4D) without inducing any cell death (data not shown). As shown in Fig. 4E, F, the increase of sphingomyelin depletion via the pretreatment with raising concentration of SMase correlated with a decreased number of apoptotic cells following Rh2 treatment. Therefore, in contrast to cholesterol removal, sphingomyelin depletion confers resistance towards Rh2-induced apoptosis, indicating that the cytotoxic activity of Rh2 depends on the membrane lipid nature.

To investigate whether the faster cytotoxic effect of Rh2 upon cholesterol depletion could result from a difference in Rh2 cell accumulation, the time course of Rh2 uptake was investigated in cells depleted or not in cholesterol. Cells were incubated with Rh2 over time

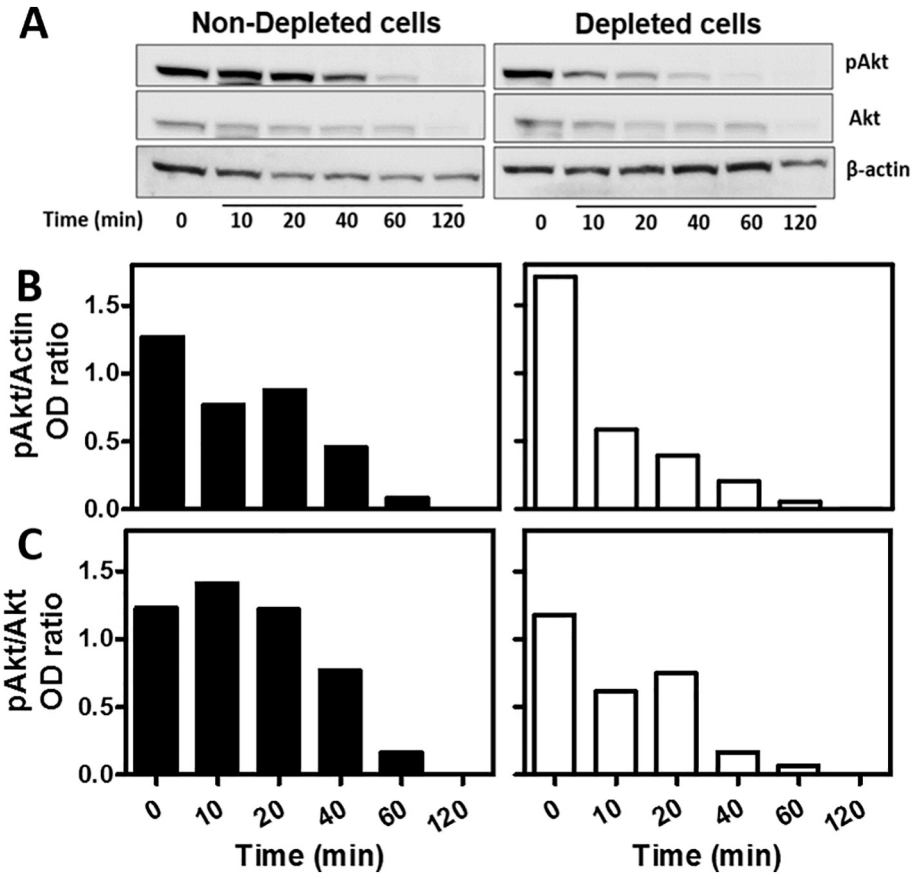

Fig. 7. Rh2 decreases the phosphorylation of Akt faster upon cholesterol depletion in U937 cells. Non-depleted (left panel) or cholesterol-depleted cells (5 mM MβCD, right panel) were incubated with 60 μM Rh2. A. Equal amounts of cell extracts were subjected to western-blot analysis for pAkt, Akt and β-actin protein. B, C. Densitometry analysis shows the band density ratios of pAkt over actin (B) and pAkt over Akt (C) in non-depleted cells (left panel, black bars) and cholesterol-depleted cells (right panel, white bars). This is a representative result from one of two independent experiments.

and the amount of Rh2 in cells was measured by HPLC MS/MS (Fig. 5). After 10 min of treatment, cholesterol-depleted cells accumulated two-fold more Rh2 as compared to non-depleted cells and this difference was maintained until 45 min. These results indicated faster cellular uptake of Rh2 upon cholesterol depletion.

To next ask whether Rh2 could affect plasma membrane biophysical properties, we measured plasma membrane fluidity, a highly regulated property, including by cholesterol. To this aim, we used DPH and TMA-DPH that respectively monitor the fluidity in the hydrophobic core and in the interfacial region of the lipid bilayer (do Canto et al., 2016). In the absence of Rh2, whereas no significant difference was observed for TMA-DPH anisotropy, DPH anisotropy value (*r*) of cholesterol-depleted cells was significantly higher than in non-depleted cells (Fig. 6), suggesting a higher rigidity in the lipid core region. Rh2 significantly increased the fluorescence polarization of DPH within 5 min in cholesterol-depleted cells but only after 30 min in non-depleted cells as compared with respective controls, suggesting that Rh2 compacted faster the lipid core region of cholesterol-depleted membranes. In contrast, Rh2 decreased the anisotropy value of TMA-DPH within 10 min in cholesterol-depleted cells and after 30 min in non-depleted cells, suggesting that Rh2 relaxed earlier the interfacial region of the lipid bilayer upon cholesterol depletion. Based on all these results, we propose that Rh2 affected faster the physical state of lipid bilayers in cholesterol-depleted cells than in non-depleted cells.

To elucidate whether membrane fluidity changes could impact on signaling pathways, we examined the effects of Rh2 on the activation of Akt, a lipid raft-associated protein kinase, which promotes cell survival and blocks the apoptotic pathways. Upon pretreatment with 5 mM MβCD and in the absence of Rh2, the levels of phospho-Akt and Akt were similar between cells depleted or not in cholesterol (Fig. 7). This observation could be at a first glance surprising since several papers show the dephosphorylation of Akt after cholesterol depletion via MβCD treatment (Calay et al., 2010; Gotoh et al., 2014). However, upon treatment with 5 mM MβCD (same concentration than our experimental condition) for 4 h, Upadhyay AK. et al. do not observe any effect neither on the Akt phosphorylation nor on the apoptosis in human breast cancer lines MCF-7 and MDA-MB-231 (Upadhyay et al., 2006). Therefore, we propose that differential incubation conditions with MβCD, i.e. dose and incubation time, could reconcile the different observations in distinct cell models. Additionally, the treatment with Rh2 decreased the level of the phosphorylated form of Akt (Ser^{473}) earlier in cholesterol-depleted cells. Regarding the disappearance of total Akt amount after 2 h of treatment with Rh2, different non-mutually exclusive explanations can be provided. Firstly, at this time, we have shown that Rh2 activated caspase-3 and could lead to the cleavage of Akt protein due to its critical role in the cell growth and its anti-apoptotic signaling properties, as suggested by Widmann C et al. (Widmann et al., 1998). Secondly, a recent study demonstrated that 60 μM Rh2 reduces Akt expression and its phosphorylation in glioma cell lines A172 without affecting the β-actin level (Li et al., 2018). Finally, it was also reported that Akt molecules can be degraded by macroautophagy (Calay et al., 2010).The dephosphorylation of Akt in a time-dependent manner resulting in the loss of its enzymatic activity could suggest the inhibition of Akt-dependent survival signaling pathways and the activation of the intrinsic apoptotic pathway by Rh2 (Franke et al., 2003).

To test for this hypothesis, apoptosis markers including loss of mitochondrial membrane potential (ΔΨ) and caspase-9 and -3 activations were investigated. ΔΨ was analyzed using the JC-1 dye. As shown in Fig. 8A, the treatment with Rh2 led to the early increase of the fluorescence intensity ratio at 525 nm (green) over 590 nm (red) upon cholesterol depletion. This result evidenced that Rh2 induced mitochondrial membrane depolarization faster in cholesterol-depleted than in non-depleted cells. Further downstream in the intrinsic apoptotic pathway, caspase-9 activity was monitored by detecting the cleavage of a specific caspase-9 substrate (Ac-LEHD-pNA). Rh2

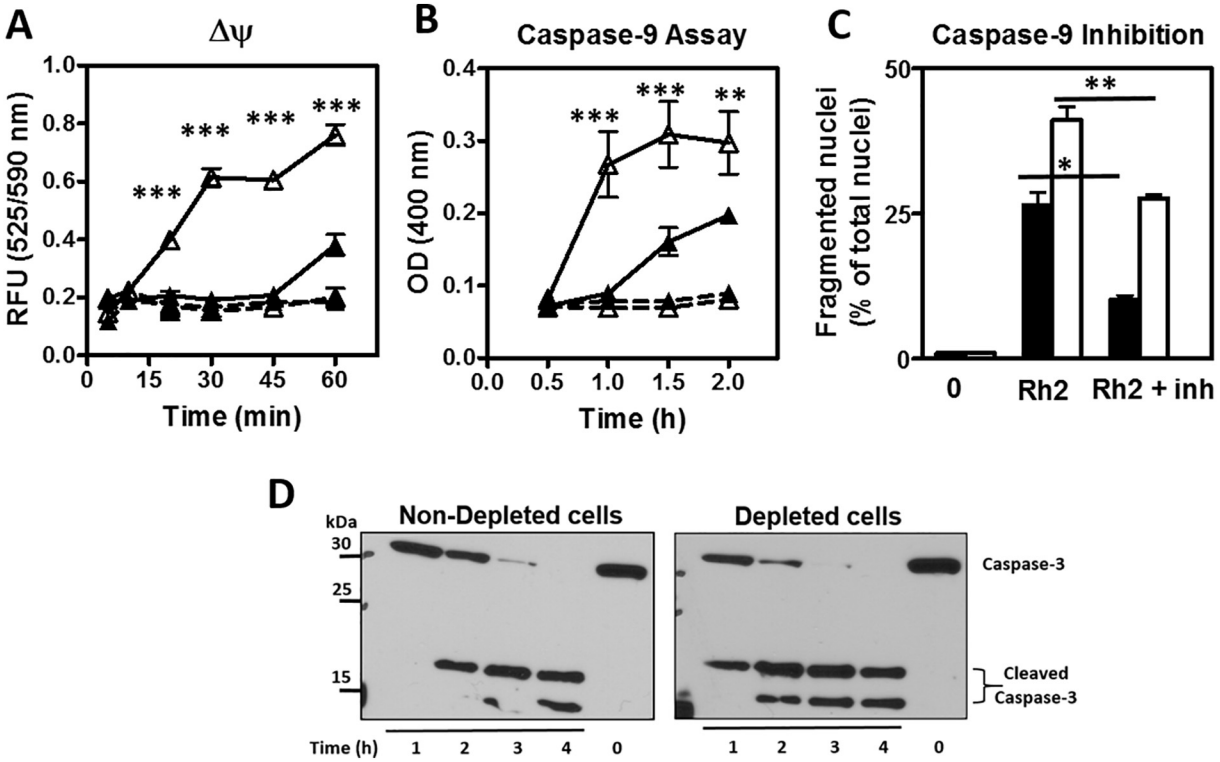

Fig. 8. Rh2 accelerates mitochondrial membrane depolarization and caspase-9 and -3 activations upon membrane cholesterol depletion in U937 cells. U937 cells were treated as at Fig. 2C. A, B. Non-depleted (closed triangles) or cholesterol-depleted cells (5 mM MβCD, open triangles) were incubated with 60 μM Rh2 (solid line) or with vehicle (dotted line) over time. A. Loss of mitochondrial membrane potential (ΔΨ) was determined by using the dye JC-1. B. Time course of caspase-9 activation was assessed by using a specific chromogenic substrate (Ac-LEHD-pNA). The experiments were repeated two times independently, each time in triplicate. Two-way ANOVA with Bonferroni post-tests to compare points for non-depleted vs depleted cells treated with Rh2. C. Non-depleted cells (black bars) or cholesterol-depleted cells (white bars) were pretreated with or without caspase-9 inhibitor (*Z*-LEHD-FMK) and then treated with 60 μM Rh2 or with vehicle for 2 h. DAPI assay was carried out as described previously. Results are means ± SEM of at least three independent experiments done in triplicate. Student's t-test was performed to compare cells depleted or not in cholesterol without and with caspase-9 inhibitor. D. The presence of active forms of caspase-3 was determined by western-blot in both cell types treated with 60 μM Rh2. This is a representative result from one of three experiments. *, $p < 0.05$; **, $p < 0.01$; ***, $p < 0.001$.

activated faster caspase-9 upon cholesterol depletion (Fig. 8B). To further address the caspase-9 involvement, cells were pretreated with specific caspase-9 inhibitor (*Z*-LEHD-FMK) followed by Rh2 treatment. The fragmented nuclei percentage was decreased more significantly by caspase-9 inhibitor in cholesterol-depleted cells as compared to non-depleted cells (Fig. 8C). Moreover, throughout the treatment with Rh2, the caspase-3 was progressively cleaved into two fragments resulting to its activation. As shown in Fig. 8D, the cleavage fragment (19 kDa) was detected after 2 h in non-depleted cells and only 1 h in cholesterol-depleted cells. As the caspase-9 activity, the caspase-3 activation was faster in cholesterol-depleted cells. Those data reported faster activation of the intrinsic apoptotic pathway by Rh2 observed via the depolarization of ΔΨ and the activation of caspase-9 and -3.

4. Discussion

Although many studies have investigated the Rh2-induced apoptosis in cancer cells (Shi et al., 2016; Lv et al., 2016; Choi et al., 2011), the role of membrane cholesterol in this process remains largely unclear. We here showed that cholesterol depletion enhanced the cellular accumulation of Rh2 in U937 cells that could result into faster Rh2-induced cytotoxicity. Based on the observation by Lorent et al. that α-hederin-induced apoptosis is reduced in cholesterol-depleted human leukemic U937 (Lorent et al., 2016), we suggest that the faster Rh2-induced cytotoxicity in cholesterol-depleted cells does not result from an unspecific mechanism due to pretreatment with MβCD. We also excluded the possibility that the observed effect could be cell-dependent, as revealed by a similar protective role of cholesterol in the Rh2-induced apoptosis in A549 and THP-1 cells.

Although we were not able to determine whether Rh2 is mostly inserted into the plasma membrane or localized inside the cell, it is tempting to speculate, based on similarity of Rh2 and cholesterol structures that Rh2 could intercalate easier and faster into the membrane of cholesterol-depleted cells by taking the place of cholesterol and modulating the membrane fluidity.

In order to determine whether the faster Rh2-induced apoptosis is specific of cholesterol depletion, we determined the cytotoxic effect of Rh2 in cells depleted or not in sphingomyelin, another abundant plasma membrane lipid exhibiting enrichment in lipid rafts. We showed that, in contrast to cholesterol depletion, sphingomyelin decrease reduced Rh2-induced apoptosis, suggesting the essential role of sphingomyelin in the cytotoxic activity of Rh2. To corroborate this idea, it has been shown that protopanaxadiol (aglycon of ginsenoside Rh2) mediates cytotoxic effects through the activation of neutral sphingomyelinase 2 leading to the hydrolysis of membrane sphingomyelins into pro-apoptotic intracellular ceramides (Park et al., 2013). Altogether, our results highlight the importance of membrane lipid composition for the ginsenoside Rh2-induced apoptosis.

To further define the interaction of Rh2 with interfacial and hydrophobic domains of the membrane, fluorescence anisotropy measurements using TMA-DPH and DPH were carried out. Both probes are located within the bilayer, with a shallower depth for TMA-DPH (do Canto et al., 2016). The steady state fluorescence anisotropy is associated to their rotational diffusion, which is sensitive to the order in the membrane. TMA-DPH fluorescence anisotropy values were not affected by cholesterol depletion in accordance with the literature, whereas

cholesterol-depleted cells showed higher rigidity in the lipid core region as compared to non-depleted cells (Prasad et al., 2009; Goodwin et al., 2005). Like cholesterol, we report here that Rh2 compacted the bilayer hydrophobic core. In addition, Rh2 relaxed the interfacial packaging of the phospholipid polar heads. These features were altered faster upon cholesterol depletion.

To investigate whether changes of the plasma membrane fluidity could potentially elicit cellular responses, we measured the effect of Rh2 on the lipid raft-associated Akt signaling and on the apoptotic pathway. We observed decreased levels of phosphorylated Akt and the activation of the intrinsic apoptotic pathway faster upon cholesterol depletion. Apoptosis markers manifested rapidly in Rh2 treated cells and only 20 to 90 min were necessary to induce the mitochondrial membrane depolarization and the activation of caspase-9 leading to apoptosis. These findings suggest that the primary action of Rh2 involved rapid pathways including phenomena such as dephosphorylation or cleavage of proteins which take less time than slower events like protein expression. Our results do not exclude the involvement of other pathways in the cytotoxic activity of Rh2 as suggest by the partial inhibition of Rh2-induced apoptosis by caspase-9 inhibitor. It has been reported that Rh2 also mediates apoptosis via the death receptor signaling leading to the activation of caspase-8 in Hela cells (Guo et al., 2014) and in A549 cells (Cheng et al., 2005).

In addition with the effect of cholesterol to delay the apoptosis induced by Rh2, two other cell effects of ginsenoside Rh2 are attributed to cholesterol-dependent mechanisms: (i) the induction of dendrite formation by Rh2 (18 μM, 2 h) is suppressed by depletion of cholesterol upon MβCD in B16 melanoma cells (Jiang et al., 2010); and (ii) a protective effect on the Aβ-induced amyloid pathology in primary neurons by Rh2 (3 μM, 12 h) is induced by reduction of cholesterol and lipid rafts (Qiu et al., 2014). These two studies could be at first glance in disagreement with the data we reported here. However, in the context of our study and the anticancerous effect of Rh2 we worked at higher concentrations (60 μM). Therefore, a differential ratio between cholesterol and Rh2 in the membrane could reconcile the different observations in distinct cell models treated with differential Rh2 concentrations.

Even if ginsenoside Rh2 was considered as a saponin like alpha-hederin or digitonin, it seems to interact differently with the lipid bilayer. Although the alpha–hederin induced cytotoxicity is well ascribed to its interaction with cholesterol, this study is the first to report that cholesterol slows down the cytotoxic activity of ginsenoside Rh2. This work highlights the need to distinguish different activities of molecules classified as saponins. Next step will be to investigate the mode of interaction of Rh2 with membranes at a molecular level using lipid monolayers and liposomes as useful models for studying membrane biophysical properties.

Acknowledgements

We thank M.C. Cambier and V. Mohymont for technical assistance and A.S. Cloos (UCL, DDUV) for guiding us in Thin Layer Chromatography experiments. S. Verstraeten is doctoral fellow of the *Télévie*. This work was supported by the Belgian *Fonds de la Recherche Scientifique* (F.S.R-FNRS).

References

Bartlett, G.R., 1959. Phosphorus assay in column chromatography. J. Biol. Chem. 234 (3), 466–468.
Billheimer, J.T., Chamoun, D., Esfahani, M., 1987. Defective 3-ketosteroid reductase activity in a human monocyte-like cell line. J. Lipid Res. 28 (6), 704–709.
Calay, D., et al., 2010. Inhibition of Akt signaling by exclusion from lipid rafts in normal and transformed epidermal keratinocytes. J. Investig. Dermatol. 130 (4), 1136–1145.
Carquin, M., et al., 2014. Endogenous sphingomyelin segregates into submicrometric domains in the living erythrocyte membrane. J. Lipid Res. 55 (7), 1331–1342.
Carquin, M., et al., 2016. Recent progress on lipid lateral heterogeneity in plasma membranes: from rafts to submicrometric domains. Prog. Lipid Res. 62, 1–24.
Cheng, C.C., et al., 2005. Molecular mechanisms of ginsenoside Rh2-mediated G1 growth arrest and apoptosis in human lung adenocarcinoma A549 cells. Cancer Chemother. Pharmacol. 55 (6), 531–540.
Choi, S., Oh, J.Y., Kim, S.J., 2011. Ginsenoside Rh2 induces Bcl-2 family proteins-mediated apoptosis in vitro and in xenografts in vivo models. J. Cell. Biochem. 112 (1), 330–340.
do Canto, A., et al., 2016. Diphenylhexatriene membrane probes DPH and TMA-DPH: a comparative molecular dynamics simulation study. Biochim. Biophys. Acta 1858 (11), 2647–2661.
Franke, T.F., et al., 2003. PI3K/Akt and apoptosis: size matters. Oncogene 22 (56), 8983–8998.
Frenkel, N., et al., 2014. Mechanistic investigation of interactions between steroidal saponin digitonin and cell membrane models. J. Phys. Chem. B 118 (50), 14632–14639.
Gamble, W., et al., 1978. Procedure for determination of free and total cholesterol in micro- or nanogram amounts suitable for studies with cultured cells. J. Lipid Res. 19 (8), 1068–1070.
George, K.S., Wu, S., 2012. Lipid raft: a floating island of death or survival. Toxicol. Appl. Pharmacol. 259 (3), 311–319.
Goodwin, J.S., et al., 2005. Ras diffusion is sensitive to plasma membrane viscosity. Biophys. J. 89 (2), 1398–1410.
Gotoh, K., et al., 2014. The antitumor effects of methyl-beta-cyclodextrin against primary effusion lymphoma via the depletion of cholesterol from lipid rafts. Biochem. Biophys. Res. Commun. 455 (3–4), 285–289.
de Groot, C., Muller-Goymann, C.C., 2016. Saponin interactions with model membrane systems - Langmuir monolayer studies, hemolysis and formation of ISCOMs. Planta Med. 82 (18), 1496–1512.
Guo, X.X., et al., 2014. p53-dependent Fas expression is critical for Ginsenoside Rh2 triggered caspase-8 activation in HeLa cells. Protein Cell 5 (3), 224–234.
Ikonen, E., 2008. Cellular cholesterol trafficking and compartmentalization. Nat. Rev. Mol. Cell Biol. 9 (2), 125–138.
Jiang, Y.S., et al., 2010. Cholesterol-dependent induction of dendrite formation by ginsenoside Rh2 in cultured melanoma cells. Int. J. Mol. Med. 26 (6), 787–793.
Kasibhatla, S., et al., 2006. Acridine orange/ethidium bromide (AO/EB) staining to detect apoptosis. CSH Protoc. 2006 (3).
Keukens, E.A., et al., 1996. Glycoalkaloids selectively permeabilize cholesterol containing biomembranes. Biochim. Biophys. Acta 1279 (2), 243–250.
Korchowiec, B., et al., 2015. Impact of two different saponins on the organization of model lipid membranes. Biochim. Biophys. Acta 1848 (10 Pt A), 1963–1973.
Kritchevsky, D., Davidson, L.M., Kim, H.K., 1973. Quantitation of serum lipids by a simple TLC-charring method. Clin. Chim. Acta 46 (1), 63–68.
Kwon, H.Y., et al., 2008. Selective toxicity of ginsenoside Rg3 on multidrug resistant cells by membrane fluidity modulation. Arch. Pharm. Res. 31 (2), 171–177.
Li, K.F., et al., 2018. Ginsenoside Rh2 inhibits human A172 glioma cell proliferation and induces cell cycle arrest status via modulating Akt signaling pathway. Mol. Med. Rep. 17 (2), 3062–3068.
Lingwood, D., Simons, K., 2010. Lipid rafts as a membrane-organizing principle. Science 327 (5961), 46–50.
Lorent, J.H., Quetin-Leclercq, J., Mingeot-Leclercq, M.P., 2014a. The amphiphilic nature of saponins and their effects on artificial and biological membranes and potential consequences for red blood and cancer cells. Org. Biomol. Chem. 12 (44), 8803–8822.
Lorent, J., et al., 2014b. Domain formation and permeabilization induced by the saponin alpha-hederin and its aglycone hederagenin in a cholesterol-containing bilayer. Langmuir 30 (16), 4556–4569.
Lorent, J.H., et al., 2016. Alpha-Hederin induces apoptosis, membrane permeabilization and morphologic changes in two cancer cell lines through a cholesterol-dependent mechanism. Planta Med. 82 (18), 1532–1539.
Lv, Q., et al., 2016. Antitumoral activity of (20R)- and (20S)-ginsenoside Rh2 on transplanted hepatocellular carcinoma in mice. Planta Med. 82 (8), 705–711.
Mollinedo, F., Gajate, C., 2015. Lipid rafts as major platforms for signaling regulation in cancer. Adv. Biol. Regul. 57, 130–146.
Park, E.K., et al., 2010. Induction of apoptosis by the ginsenoside Rh2 by internalization of lipid rafts and caveolae and inactivation of Akt. Br. J. Pharmacol. 160 (5), 1212–1223.
Park, B., et al., 2013. Neutral sphingomyelinase 2 modulates cytotoxic effects of protopanaxadiol on different human cancer cells. BMC Complement. Altern. Med. 13, 194.
Prasad, R., et al., 2009. Membrane cholesterol depletion from live cells enhances the function of human serotonin(1A) receptors. Biochem. Biophys. Res. Commun. 389 (2), 333–337.
Qi, L.W., Wang, C.Z., Yuan, C.S., 2011. Ginsenosides from American ginseng: chemical and pharmacological diversity. Phytochemistry 72 (8), 689–699.
Qiu, J., et al., 2014. Ginsenoside Rh2 promotes nonamyloidgenic cleavage of amyloid precursor protein via a cholesterol-dependent pathway. Genet. Mol. Res. 13 (2), 3586–3598.
Servais, H., et al., 2006. Gentamicin causes apoptosis at low concentrations in renal LLC-PK1 cells subjected to electroporation. Antimicrob. Agents Chemother. 50 (4), 1213–1221.
Shi, Q., et al., 2016. Anticancer effect of 20(S)-ginsenoside Rh2 on HepG2 liver carcinoma cells: activating GSK-3beta and degrading beta-catenin. Oncol. Rep. 36 (4), 2059–2070.
Simons, K., Ikonen, E., 1997. Functional rafts in cell membranes. Nature 387 (6633), 569–572.
Simons, K., Sampaio, J.L., 2011. Membrane organization and lipid rafts. Cold Spring Harb. Perspect. Biol. 3 (10), a004697.
Sudji, I.R., et al., 2015. Membrane disintegration caused by the steroid saponin digitonin is related to the presence of cholesterol. Molecules 20 (11), 20146–20160.
Tsuchiya, H., 2015. Membrane interactions of phytochemicals as their molecular

mechanism applicable to the discovery of drug leads from plants. Molecules 20 (10), 18923–18966.
Upadhyay, A.K., et al., 2006. Methyl-beta-cyclodextrin enhances the susceptibility of human breast cancer cells to carboplatin and 5-fluorouracil: involvement of Akt, NF-kappaB and Bcl-2. Toxicol. Appl. Pharmacol. 216 (2), 177–185.
Widmann, C., Gibson, S., Johnson, G.L., 1998. Caspase-dependent cleavage of signaling proteins during apoptosis. A turn-off mechanism for anti-apoptotic signals. J. Biol. Chem. 273 (12), 7141–7147.
Yi, J.S., et al., 2009. Ginsenoside Rh2 induces ligand-independent Fas activation via lipid raft disruption. Biochem. Biophys. Res. Commun. 385 (2), 154–159.
Zidovetzki, R., Levitan, I., 2007. Use of cyclodextrins to manipulate plasma membrane cholesterol content: evidence, misconceptions and control strategies. Biochim. Biophys. Acta 1768 (6), 1311–1324.